CrossMark

REVIEW ARTICLE

Microbubbles used for contrast enhanced ultrasound and theragnosis: a review of principles to applications

Hohyeon Lee[1] · Haemin Kim[2] · Hyounkoo Han[1] · Minji Lee[1] · Sunho Lee[1] ·
Hongkeun Yoo[1] · Jin Ho Chang[2,3] · Hyuncheol Kim[1,2]

Abstract Ultrasound was developed several decades ago as a useful imaging modality, and it became the second most popular diagnostic tool due to its non-invasiveness, real-time capabilities, and safety. Additionally, ultrasound has been used as a therapeutic tool with several therapeutic agents and in nanomedicine. Ultrasound imaging is often used to diagnose many types of cancers, including breast, stomach, and thyroid cancers. In addition, ultrasound-mediated therapy is used in cases of joint inflammation, rheumatoid arthritis, and osteoarthritis. Microbubbles, when used as ultrasound contrast agents, can act as echo-enhancers and therapeutic agents, and they can play an essential role in ultrasound imaging and ultrasound-mediated therapy. Recently, various types of ultrasound contrast agents made of lipid, polymer, and protein shells have been used. Air, nitrogen, and perfluorocarbon are usually included in the core of the microbubbles to enhance ultrasound imaging, and therapeutic drugs are conjugated and loaded onto the surface or into the core of the microbubbles, depending on the purpose and properties of the substance. Many research groups have utilized ultrasound contrast agents to enhance the imaging signal in blood vessels or tissues and to overcome the blood–brain barrier or blood-retina barrier. These agents are also used to help treat diseases in various regions or systems of the body, such as the cardiovascular system, or as a cancer treatment. In addition, with the introduction of targeted moiety and multiple functional groups, ultrasound contrast agents are expected to have a potential future in ultrasound imaging and therapy. In this paper, we briefly review the principles of ultrasound and introduce the underlying theory, applications, limitations, and future perspectives of ultrasound contrast agents.

Keywords Microbubble · Ultrasound · Contrast agent · Theragnostics · Sonoporation

✉ Jin Ho Chang
jhchang@sogang.ac.kr

✉ Hyuncheol Kim
hyuncheol@sogang.ac.kr

1 Department of Chemical and Biomolecular Engineering, Sogang University, 35 Baekbeom-ro, Mapo-gu, Seoul 04107, Republic of Korea

2 Department of Biomedical Engineering, Sogang University, 35 Baekbeom-ro, Mapo-gu, Seoul 04107, Republic of Korea

3 Sogang Institute of Advanced Technology, Sogang University, 35 Baekbeom-ro, Mapo-gu, Seoul 04107, Republic of Korea

1 Introduction

Medical ultrasound imaging has been firmly established as a critical diagnostic tool due to its real-time capabilities, portability, safety, and functional imaging capabilities. These features are prominent advantages over other imaging modalities, including magnetic resonance imaging (MRI) and computer tomography (CT), making ultrasound imaging the second most popular imaging modality in the medical market. According to a survey in 2015, the worldwide market for ultrasound imaging devices will reach approximately 8 billion dollars by the year 2020 [1]. The major clinical applications of ultrasound imaging are cardiology (abdominal, thyroid, heart, and blood vessel-related) and obstetrics, mainly for the diagnosis of various diseases including cancers. Due to technical advancements, ultrasound has recently drawn attention in the fields of brain imaging [2, 3], fusion imaging [4–8], cellular

🙂 Springer

biophysics [9–11], and theragnosis [12–15]. Contrast agents are a big part of this trend as they allow for maximizing the usefulness of ultrasound. Among the various contrast agents available, microbubbles have been developed for contrast enhancement of ultrasound imaging and theragnosis [16].

Microbubbles generally consist of a shell that surrounds a core gas. Materials that often comprise microbubble shells include lipids [17], proteins [18], and polymers [19]. Air [20], nitrogen [21], and perfluorocarbon [22] are typically used as the core gas (Fig. 1). To increase the contrast resolution of an ultrasound image, microbubbles exposed to a certain frequency experience a resonance phenomenon [23–26]. The resonant frequency of microbubbles with diameters of 1–7 μm lies within the 2–15 MHz range, and this is the ultrasound frequency range used in clinical diagnosis [27]. When used as a contrast agent, microbubbles can be detected by an ultrasound device when they possess acoustical characteristics that differ from the surrounding medium. The microbubbles act as echo-enhancers by essentially the same mechanism of echo-scattering found in all other cases of diagnostic ultrasound: by increasing ultrasound impedance such that there is a mismatch between the microbubbles and the surrounding tissues.

Theragnostic applications are achieved through the mechanisms of cavitation [28] and sonoporation [29], which are the combined effects of ultrasound and microbubbles. This will be discussed in detail in later sections. Sonoporation refers to a technique capable of controlling drug delivery efficiency by maximizing the drug permeability of surrounding tissues or cells using a reaction mechanism between microbubbles and ultrasonic waves [30, 31]. In addition, it is possible to not only deliver drugs together with very high efficiency, but also to minimize the adverse effects via time- and site-specific therapeutic strategies. Furthermore, the microbubbles not only have a therapeutic effect when combined with ultrasound as mentioned above, but also can themselves act as the drug delivery vehicles [32–34]. For example, for

microbubbles composed of lipids, hydrophobic anticancer drugs can be very efficiently loaded onto the hydrophobic tail of the lipid found between the gas core and the shell [35]. Thus, the loaded drug can be safely delivered to the target tissue without being attacked by various enzymes present in the blood and can then be released in response to ultrasonic waves as an external stimulus-triggered drug release strategy [36].

In this review, we introduce the basic principles of microbubbles as ultrasound contrast agents and provide a brief description of commercialized products, as well as research on and applications of microbubbles and ultrasound for the treatment of various diseases. In particular, we focus on the study of microbubbles used in the treatment of various diseases and discuss the limitations and development directions of the present microbubble technology.

2 Commerical ultrasound contrast agents

Microbubbles with a size of 1–10 μm are common ultrasound contrast agents, and many kinds of microbubbles have been developed for use in ultrasound imaging and as a medical treatment technique [37, 38]. Microbubbles consist of a shell and a gas core. As technology gradually develops, the creation of small microbubbles with uniform size became possible [39]. For example, small or highly elastic microbubbles can pass through capillary vessels, thereby becoming able to circulate to the entire body and possibly reach the target organs [40]. For this reason, many studies have tested several shell materials and core gases with high molecular weights and low solubilities. Shell materials like proteins, lipids, and polymers disperse in an aqueous solution with a surfactant, or a combination of two substances can be used for stability [41]. A representative sample of commercially used microbubbles including Levovist®, Definity®, Optison®, Sonazoid® and SonoVue® [42–46] are listed in the order of discussion in the following

Fig. 1 Schematic illustration of a microbubble. **a** Representative illustration of a lipid shell, **b** representative illustration of a protein shell, **c** representative illustration of a polymer shell. Various kinds of gas (ex. perfluorocarbon, nitrogen, air) can be used in various kind of shell
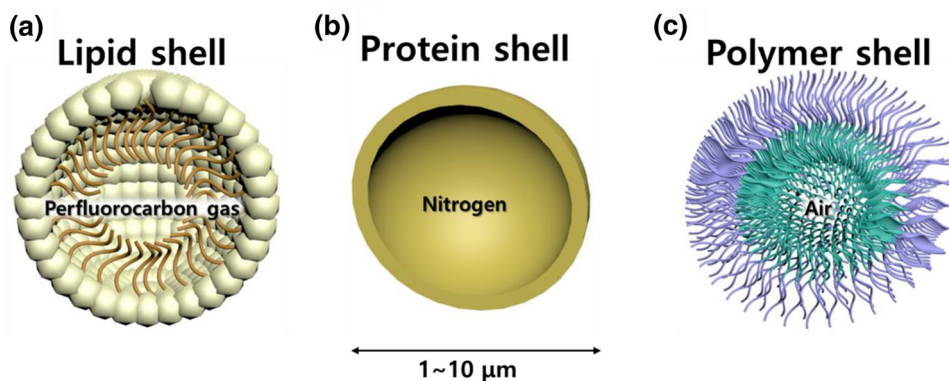
subsections. The physical properties of these microbubbles are also summarized in Table 1.

2.1 Levovist®

Levovist microbubbles are the first generation of ultrasound contrast agents. They have a shell composed of 99.9% galactose, which is biocompatible, and a core of 0.1% palmitic acid mixed with air [47]. Levovist microbubbles have harmonic signals that enhance ultrasound imaging by decreasing noise signals. These microbubbles can only be destroyed during high acoustic power harmonic imaging. So, a transducer with low acoustic power is somewhat inadequate for use with Levovist microbubbles [48].

2.2 Optison®

Optison microbubbles consist of an octafluoropropane core covered by an outer protein shell composed of human serum albumin. Together with galactose, microbubbles with albumin shells have been consistently studied because of their stability in coronary blood flow or systemic hemodynamics [49–51]. Although albumin-based microbubbles are phagocytosed by Kupffer cells, which are a component of the liver, they still retain their acoustic properties. Kupffer cells phagocytose contrast agents, and the imaging difference is so clearly evident between normal tissue and cancer tissue that lesion location can be precisely identified [49, 52]. This phenomenon enables continuous imaging during and after the microbubbles circulate throughout the entire body [53].

2.3 SonoVue®

SonoVue microbubbles consist of an SF_6 core covered by a phospholipidic monolayer outer shell, which has a low solubility [54, 55]. SonoVue microbubbles can be restored after lyophilization and has low cytophagy property to peripheral cells. Above all, SonoVue microbubbles are stable in the presence of several surfactants, such as polyethylene glycol, phospholipids, and palmitic acid, and can be maintained in the vial for at least 6 h [56]. Furthermore, because SF_6 has a low solubility, SonoVue microbubbles have high and prolonged stability in the peripheral blood, which improves harmonic behavior at low acoustic power [57].

2.4 Definity®

Definity microbubbles consist of an octafluoropropane core covered by a shell composed of various lipids. This product is currently distributed mainly in Europe and North America. The use of octafluoropropane facilitates the use of low acoustic power modes. Additionally, due to the use of several lipids in the shell, these microbubbles are highly stable when exposed to ultrasound [58].

2.5 Sonazoid®

Sonazoid microbubbles consist of a perfluorobutane core covered by a lipid shell. Perfluorocarbon has low reactivity with other molecules because of its strong carbon–fluorine bonding. Sonazoid microbubbles are stable for a longer time and have fewer side effects compared to other microbubbles [52]. Additionally, Sonazoid has been used for the detection of focal liver lesions and can diagnosis malignant tumors in the liver [59]. Similar to the Optison microbubbles, Sonazoid microbubbles are also used with Kupffer cells.

3 Theory of ultrasound imaging with microbubbles

Microbubbles were invented for use as an ultrasound contrast agent to enhance image resolution to distinguish vessels clearly and minimize noise and background signals (Fig. 2) [60]. In this section, we will review the theory of microbubbles within the framework of ultrasound imaging.

3.1 Ultrasound imaging with microbubbles

Since Gramiak and Shah discovered that an ultrasound signal is altered when passing through the saline that is injected into the micro-vessels [61], microbubbles have been studied as a way to enhance ultrasonic signals. A shelled microbubble resonates in response to a transmitted

Table 1 Type and physical properties of ultrasound contrast agents

Name	Shell	Core gas	Mean diameter (μm)
Levovist®	Galactose/palmitic acid	Air	2–8
Optison®	Human albumin	Octafluoropropane	1.0–2.25
SonoVue®	Lipid	Sulfur hexafluoride	3.0
Definity®	Lipid	Octafluoropropane	2.5
Sonazoid®	Lipid	Perfluorobutane	3.2

Fig. 2 Ultrasound images using microbubbles **a** in vitro images of microbubbles prepared via a microfluidic system and **b** in vivo images of a tumor before and after injection of microbubbles
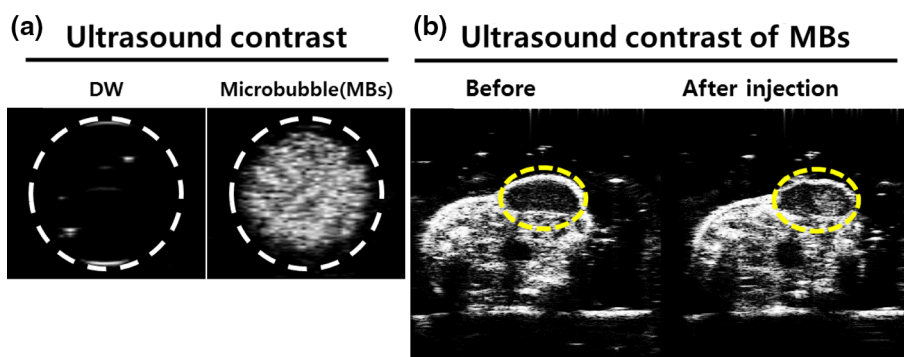
acoustic wave, and its linear resonant frequency f_r is determined by its radius r, the density of the surrounding medium ρ, the equilibrium pressure inside the microbubble p_e, the polytropic index of gas κ, the shear modulus of the shell G_s, and instantaneous shell thickness d_s as follows as follows [62].

$$f_r = \frac{1}{2\pi r} \sqrt{\frac{3\kappa p_e + 12 G_s \frac{d_s}{r}}{\rho}} \tag{1}$$

Equation (1) indicates that the characteristics of the shell influence the resonant frequency of a microbubble although the resonant frequency is typically inversely proportional to the size of the microbubble. In general, the resonant frequency of encapsulated microbubbles is higher than that of gas bubbles at a given size. Note that an ultrasound transducer with an operating frequency similar to the resonant frequency of microbubbles is generally used in clinics to maximize the energy of echoes from the microbubbles. As the amplitude of the transmitted ultrasound wave increases, the microbubble nonlinearly responds; it expands well in response to the rarefactional pressure of the ultrasound wave but then contracts poorly in response to the wave's compressional pressure. As such, the microbubble generates a harmonic frequency components of transmitted ultrasound and their amplitude is considerably higher than that of the harmonic frequencies produced by the tissues when imaged. When the acoustic pressure exceeds some threshold, the microbubble bursts. This is called the cavitation effect. This threshold is associated with the amplitude of peak rarefactional pressure generated by an ultrasound transducer.

Due to the high echogenicity of microbubbles even under low MI, contrast-enhanced ultrasound images can be acquired when microbubbles are used. After microbubbles are administered to a blood vessel by intravenous injection, they are diffused to blood vessels and organs. Thus, it is possible to acquire contrast-enhanced ultrasound images of blood vessels and organs (e.g., the heart). Therefore, with this imaging technique, the accuracy with which cancer [63], metastasis [64], and cardiovascular diseases [65] are

diagnosed can be improved. Additionally, the nonlinear behavior of microbubbles (i.e., generation of harmonic frequency components) can be used to increase the spatial resolution of ultrasound images; the center frequency and spectral bandwidth of ultrasound are the major factors determining the spatial resolution. The harmonic components generated by microbubbles have higher frequency than incident ultrasound (or their resonant frequency). For high spatial resolution images, therefore, one of harmonic components is extracted from the echoes received by an ultrasound transducer and used to construct an image, called ultrasound harmonic imaging. In fact, this harmonic imaging technique was developed to simultaneously improve both spatial and contrast resolutions of tissue images by using the nonlinear behavior of ultrasound in tissue [66, 67]. However, the improvement of image quality by the harmonic imaging technique is limited in the case of general tissue imaging because only the second harmonic component is available to construct ultrasound images of the tissues. This is because the other harmonic components induced in the tissue have a very low amplitude. In contrast, because the amplitude of the third or even higher harmonic components generated by microbubbles is high enough for ultrasound imaging, super-harmonic imaging [68] and second harmonic imaging are viable [69].

Recently, it has been reported that the ultrafast ultrasound imaging method using plane waves is capable of detecting the slow movement of microbubbles with sub-wavelength size [3]. Since the frame rate of the plane wave imaging method is higher than 500 frames per second, each frame can contain the information about microbubble displacement smaller than the wavelength and displacement vectors are obtained by comparing the positions of microbubbles in adjacent frame images. Velocity vectors corresponding to the speed of blood in vessels can be calculated from the displacement vectors based on the prior knowledge of the time interval between the image frames. The velocity map provides a super-resolution image of blood vessel as well as information about blood velocity in the vessel.

4 Theory of therapeutic effects of microbubbles

Microbubbles have also recently been recognized for their therapeutic abilities. These attractive characteristics led many researchers to study the mechanism of microbubbles and use them in their research. In this section, underlying theories of ultrasound and microbubbles as therapeutic agents will be reviewed [70].

4.1 Cavitation

One of the most attractive capabilities of ultrasound-mediated therapy is the enhancement of the cell membrane's permeability, which is induced by microbubble cavitation (Fig. 3) [32]. In general, the cavitation of microbubbles by ultrasonic waves is a phenomenon involving both oscillation and destruction, thereby forming jet streaming and physical effects on surrounding tissues. However, here we will focus only on aspects related to the therapeutic effect of ultrasound-induced microbubble cavitation. Especially, it is classified into stable and inertial cavitation due to the degree of deformation according to ultrasonic intensity applied to the microbubble. Stable cavitation induces a pushing and pulling of the cell membrane that generates microstreaming near the adjacent cells, resulting in increased permeability of the cell membrane. On the other hand, inertial cavitation can induce collapse of the microbubble and jet streaming towards the cell membrane, which can make temporary pores in the cell membrane [28, 29, 71]. Furthermore, when a fluid with gas bubbles is irradiated by an acoustic field and the gas bubbles are under the primary radiation force experienced by single particles, microbubbles can be transported across the cell membrane.

The application of cavitation as a therapeutic strategy will be discussed in the following section.
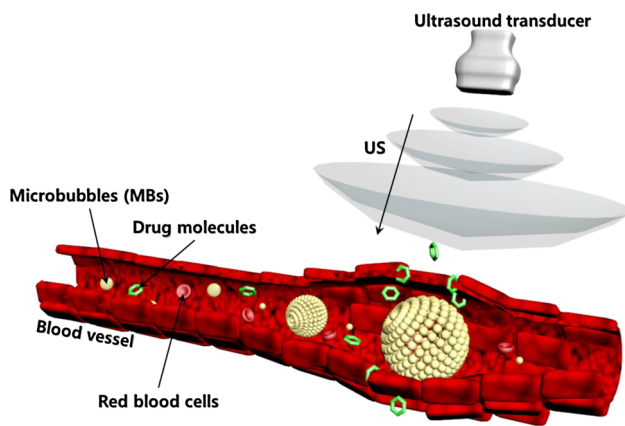
4.2 Sonoporation effect

When a microbubble collapses via inertial cavitation, surrounding cell or tissue membranes are ruptured due to the generated jet streaming and shock wave (Fig. 4) [29, 72]. Many researchers have investigated the mechanism of sonoporation [73, 74], though the exact mechanism is still unclear. Recently, Fan et al. [75] reviewed potential mechanisms of sonoporation classified by several acoustic properties. Sonoporation allows the microbubble itself to behave as a therapeutic agent and to deliver therapeutic agents to the target cells or blood vessels at the site of ultrasound irradiation by generating temporary pores in cell membranes [76]. It is a temporary phenomenon and can extravasate large molecules such as DNA so that they pass through extravascular tissue [77]. Using the sonoporation effect of microbubbles for disease therapy has many advantages. Injecting microbubbles intravenously can minimize drug side effects that may cause nonspecific delivery of drugs into healthy organs because the microbubbles only collapse in specific diseased areas due to focused ultrasound irradiation. Furthermore, this technique can improve the bioavailability of drugs due to effective drug delivery, thereby requiring a lower dosage [78].

4.3 Studies on factors affecting sonoporation effect

Kooiman et al. [79] have demonstrated that microbubbles that are conjugated with antibodies, referred to as targeted

Fig. 3 The cavitation of a microbubble according to incident acoustic pressure
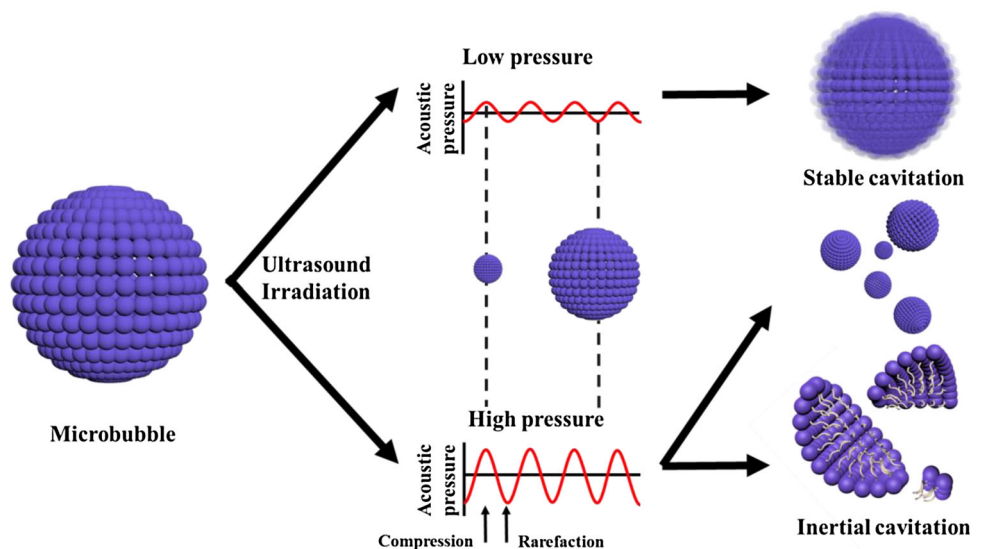
Fig. 4 Therapeutic use of the sonoporation effect of microbubble

microbubbles, amplify the sonoporation effect under relatively low peak negative acoustic pressures. In the example of epithelial cancer, microbubbles become attached to the cell membrane due to the affinity between the antibody and CD31, which is expressed on the surface of all endothelial cancer cells. This results in an improved sonoporation effect on the target cells compared to those in a control group. As a result, 30, 20, and 83% of the cells had taken up fluorescent dye at 80, 120, and 200 kPa, respectively. This result also demonstrates that the peak negative acoustic pressure also affects the sonoporation effect when delivering therapeutic agents. Another group, Karshafian et al., showed similar results regarding how the sonoporation effect is influenced by the peak negative pressure [80]. Under ultrasound irradiation, cells accommodate various molecule sizes depending on the peak negative pressure. They showed that the sonoporation effect of Definity® and Optison® microbubbles causes changes in the ability of the cell to uptake FITC-dextran with different molecular weights according to different peak negative pressures. These results showed that larger-sized FITC-dextran (from 10 kDa to 2 MDa) can enter the cells when the acoustic pressure increases from 125 to 570 kPa. Additionally, another factor affecting sonoporation has also been proposed. Liao et al. showed that the evaluations of the penetration depth was studied with microbubbles of different sizes (1.4–3.5 μm). As a result, when exposing the ultrasound of the same intensity, larger microbubbles result in more uniform penetration depths, which demonstrates that large microbubbles can increase the effective drug delivery and improve the sonoporation effect [81].

5 Therapeutic applications of microbubbles

Microbubbles are also used in therapeutic applications based on the intrinsic sonoporation ability of the encapsulated drugs. In this section, various therapeutic

applications of microbubbles are summarized, organized by target tissues; blood–brain barrier, cancers, cardiovascular system. First, cavitation and sonoporation are used for overcoming biological drug delivery barriers, such as the blood–brain barrier. Next, several studies on microbubble sonoporation effects as cancers and cardiovascular disease therapy will be reviewed.

5.1 Blood–brain barrier

The blood–brain barrier (BBB) is a physical barrier composed of endothelial cells linked by tight junctions. The BBB selectively transports several molecules into the central nervous system (CNS) and protects the brain from external substances, such as toxic compounds or pathogens [82]. To achieve effective drug delivery, it is important to loosen the tight junctions between the epithelial cells. Recently, microbubbles coupled with ultrasound exposure have been studied for opening the BBB and delivering drugs [36, 83, 84]. Hynynen et al. [85] showed that local and reversible BBB disruption by non-invasive FUS results in focal disruption of the BBB, necessitating future research on the brain and diagnostic and therapeutic effects. Also, Konofagou et al. showed that local and reversible BBB opening by FUS in non-human primates (NHP). Microbubble's diffusion patterns revealed important information of the FUS-induced BBB opening following the patterns of the underlying brain structures [86]. Stable cavitation is thought to be the major mechanism of opening the BBB. Mechanical and shear stress, generated by stable cavitation of microbubbles, increases the permeability of blood vessel walls in the brain, resulting in the reduction of tight junctions between the vascular endothelial cells. Furthermore, microbubbles under ultrasound exposure affect the efflux transporters in the BBB, which act as a functional barrier [87]. In a study of the BBB in rat brains, Cho et al. revealed a correlation between P-gp expression and the opening of the BBB. Although there are some limitations, such as the time difference between P-gp fluorescence imaging and ultrasound irradiation, the results showed that ultrasound and microbubbles inhibited expression of P-gp. Although the exact mechanism was not demonstrated in this study, it suggests that ultrasound and microbubbles can potentially be used to control the drug efflux ability of the BBB.

5.2 Cancers

Since the applicability of ultrasound contrast agents has been spotlighted, ultrasound contrast agents has attracted great attention in cancer diagnostic and therapy. Ultrasound contrast agents including microbubbles with lipid-, protein-, and polymer-based shells have been developed and also

used as drug loaded-therapeutic agent by many groups. These microbubbles were used as ultrasound-guided cancer therapy. For examples, numerous studies have reported that ultrasound-guided cancer therapy using microbubbles has high potentials to enhance the therapeutic effects on lethal cancer types such as breast cancer [88], liver cancer [89–91], and pancreatic cancer [92, 93].

Sorace et al. [94] developed contrast-enhanced ultrasound and targeted microbubble for assessing the early tumor response to antiangiogenic therapy in breast cancer. To visualize molecular US imaging of angiogenic markers in breast cancer, multitargeted microbubbles were fabricated. Antibodies against mouse $\alpha_v\beta_3$ integrin, P-selectin, and VEGFR2 were conjugated to the surface of microbubbles. In this research, multitargeted microbubbles showed that the evaluation and assessment of the early response to antiangiogenic treatment can be utilized in in vivo breast cancer animal model.

In addition, other research groups studied the use of nanomedicine technology combined with ultrasound-mediated microbubble destruction techniques for cancer therapy. Among them, Bai et al. [88] showed that the enhanced therapeutic effect of Adriamycin on multidrug resistant breast cancer was achieved by combining siRNA silencing ABCG2-loaded mPEG-PLGA-PLL nanoparticles (PEAL NPs) and ultrasound-targeted microbubble destruction. Multidrug resistance, the principal mechanism by which many cancers develop resistance to chemotherapy, is induced by a novel protein, ABCG2 [95], which is a member of the ATP-binding cassette (ABC) transporter family [96]. To overcome the drug resistance obstacle in breast cancer therapy, Bai M et al. fabricated the siRNA silencing ABCG2-loaded mPEG-PLGA-PLL nanoparticles (PEAL NPs) and then combined these developed nanoparticles with ultrasound-targeted microbubble destruction (UTMD). Microbubbles facilitate the enhanced penetration of PEAL NPs into the multidrug resistant breast cancer cells. Therefore, more anti-ABCG2 siRNA, dissociated from PEAL NPs, was accumulated in the cell's cytosol and showed an enhanced gene silencing effect compared to PEAL NP without UTMD. This resulted in increased Adriamycin accumulation in multidrug resistant breast cancer cells. Ultimately, this therapeutic strategy exhibited effective, feasible inhibition of drug resistance in breast cancer.

The followings are examples of pancreatic cancer. Kotopoulis et al. [92] showed that a custom-made ultrasound transducer has been developed to induce the sonoporation effect in pre-clinical studies and to create a bioluminescent model of pancreatic adenocarcinoma (PA). The aim of this study was to increase the delivery of gemcitabine to pancreatic tumors by confirming the effect of sonoporation for local cancer therapy in MIA PaCa-2

human pancreatic cancer cells via the inoculated mice model. The research showed in detail that a custom-made single-element ultrasound transducer can validate the beam profile, with a focus that is 4.0 mm in diameter and 22.0 mm in length to induce sonoporation. The therapeutic transducer can control the sound field with high precision in the focused treatment area. In this research, the tumors of inoculated mice (n = 10) were measured using 3D ultrasound and bioluminescent imaging to evaluate the safety and efficacy of sonoporation of gemcitabine combined with microbubbles. As a result, the combined treatment group showed a significant therapeutic effect compared to the control (untreated) and gemcitabine groups. Based on these results, ultrasound-guided cancer therapy with microbubbles exhibited remarkable therapeutic efficacy.

Moreover, the Du research group used combined nanomedicine and ultrasound-mediated microbubble destruction techniques to enhance the therapeutic effect on pancreatic cancer [93]. Due to the limitations of conventional chemotherapeutic treatment, pancreatic cancer is considered one of the most lethal human malignancies among numerous cancers. This research showed that pancreatic cancer-targeting, three-block copolymer methoxy polyethylene glycol-polylacticco-glycolic acid-polylysine (mPEG-PLGA-PLL) NPs, which were modified with anti CA19-9 antibodies and encapsulated paclitaxel (PTX) and combined with ultrasound-mediated microbubble destruction (UMMD) significantly increased the cellular uptake in vitro and drug retention in vivo, suggesting a promising strategy for cancer therapy. Their study demonstrated that UMMD technology could significantly increase cellular uptake in vitro and enhance the EPR effect in vivo, thereby improving the therapeutic efficacy of pancreatic cancer therapy.

In addition, liver cancer is also one of the major target tumors for treatment with microbubbles and ultrasound. As in the previous case of breast and pancreatic cancers, a strategy referred to as UTMD or UMMD can be equally applied to liver cancer [91].

5.3 Cardiovascular system

Stroke and myocardial infarction are among the most common causes of death [97, 98]. One of the first therapeutic strategies developed using ultrasound and microbubbles was targeted at treatment of these cardiovascular diseases. One major therapeutic strategy targeted at the cardiovascular system is sonothrombolysis, whose underlying principle is based on cavitation effects [99]. Sonothrombolysis has been studied as a treatment for both acute ischemic stroke and acute myocardial infarction. Although ultrasound itself is well known to increase the

dissolution rate of clots because elimination of the no-re-flow region in the circulatory bed results in the recovery of blood flow, microbubbles can be incorporated into cardiovascular-therapeutic applications of ultrasound for increased efficiency via the mechanisms of cavitation and sonoporation.

In sonothrombolysis, the thrombus, which causes cardiovascular diseases, is one of the main targets. Fibrinolytic drugs, such as streptokinase, which is one of the plasminogen activators (PAs), are used in the treatment of thrombi. However, PAs can induce side effects (e.g., bleeding complications and neurotoxicity) during pharmacological therapy of thrombi, and a rapid, non-invasive imaging technology is not available. Wang et al. [100] investigated a novel technology in which thrombus-targeting microbubbles, which have fibrinolytic drugs on the surface, can overcome this problem. Specifically, anti-GPIIb/IIIa single-chain antibodies, which bind specifically to the main fibrinogen/fibrin receptor-mediating platelet aggregation, and single-chain urokinase plasminogen activators are conjugated onto the microbubble for enhanced and localized delivery of therapeutic agents. Using this technique, they reduced the size of the thrombus via ultrasound imaging without prolonging bleeding time.

Additionally, Hagisawa et al. [101] demonstrated significant improvements in ultrasonic thrombus disruption in vitro and in vivo via thrombus-targeted perfluorocarbon-bubble liposomes (BLs) and an external low-frequency ultrasound system. Thus, it is highly possible that a non-invasive therapy combining low-frequency ultrasound with thrombus-targeted BLs could be developed. Consequently, sonothrombolysis and drug delivery methods have been reported to recanalize canine iliofemoral and coronary arteries without tissue damage. These studies demonstrate that clinically available diagnostic low-frequency ultrasound systems can be used for thrombus dissolution with thrombus-targeted microbubbles.

6 Limitations of microbubbles

Microbubbles take center stage in ultrasound imaging and therapy because of their sensitive contrast and therapeutic efficiency. However, stability limitations, caused by diffusion of the core gas across the shell, still exist. Many researchers have tried to overcome this limitation using mixed materials, such as PEG, for shells or by blending core gases such as nitrogen and perfluorocarbon [102]. Improved shell stability can substantially enhance microbubble functionality and in vivo therapeutic application strategies. Furthermore, the large size distribution of microbubbles presents a limitation for utilizing advanced ultrasound imaging via resonant frequency properties. Due

to the large size distribution of microbubbles, a weak subharmonic response is induced at high frequency, resulting in subharmonic imaging with a low sensitivity [103]. Another limitation of the microbubble is the scale of its size when used in drug delivery to tumor tissues. The micrometric proportions of microbubbles limit their ability to penetrate through the intercellular junctions. Consequently, most microbubble applications are limited to blood vessels.

7 Future perspective of microbubbles

Currently, microbubble size is delicately controlled via several methods, including centrifugation [104] and microfluidics [105]. Microbubble size is a significant property that merits future research (e.g., resonance frequency [106]). If research on size-dependent properties is broadened, subsequent mechanistic studies will follow. Furthermore, to overcome the limitation about microbubble size, many researchers have developed gas-generating or evaporation strategies, in which nanometer-scale particles or bubbles containing liquid can evaporate under biological conditions or as an external stimuli, such as a laser, increases temperature [107]. Min et al. [108] have constructed doxorubicin-loaded calcium carbonate ($CaCO_3$) hybrid nanoparticles (DOX-$CaCO_3$-MNPs) through a block copolymer templated in situ with the mineralization approach. This nanoparticle can generate CO_2 bubbles at weak acidic tumoral pH (pH 6.8-7.2) levels and release loaded drugs into tumor tissues. Consequently, passive tumor targeting is expected due to the enhanced permeability and retention (EPR) effect of nanoparticles, resulting in efficient drug delivery to tumor sites and subsequent ultrasound imaging by the generated gas. In this review, we focused on the therapeutic application through the sonoporation effect of microbubbles, but studies on the functionalization of microbubbles, such as the above example, are also actively conducted. These studies such as coating microbubbles with nanoparticles [109], US/MR dual-modal microbubbles [19], microbubbles for targeted imaging [110] can enhance the potential to overcome the limitations of microbubbles and extend their applications.

8 Conclusion

Overall, microbubbles, as functional ultrasound contrast agents, have enormous potential for use in advanced ultrasound imaging and therapeutic strategies. Beyond the currently used basic ultrasound contrast agents, many researchers have developed functionalized microbubbles for specific molecule-targeted imaging and therapeutic use

in the treatment of various diseases. Recent studies on the combined effects of ultrasound and microbubbles have shown positive results for clinical translation. Even considering the limitations mentioned in the previous section, it is highly expected that advanced next-generation microbubbles will be used clinically in the near future.

Compliance with ethical standards

Conflict of interest The authors report no financial or other conflict of interest relevant to the subject of this article.

References

1. Castle J, Feinstein SB. Drug and gene delivery using sonoporation for cardiovascular disease. Ther Ultrasound. 2016;880:331–8.
2. Mace E, Montaldo G, Cohen I, et al. Functional ultrasound imaging of the brain. Nat Methods. 2011;8(8):662–4.
3. Rrico CE, Pierre J, Pezet S, et al. Ultrafast ultrasound localization microscopy for deep super-resolution vascular imaging. Nature. 2015;527(7579):499–502.
4. Montilla LG, Olafsson R, Bauer DR, et al. Real-time photoacoustic and ultrasound imaging: a simple solution for clinical ultrasound systems with linear arrays. Phys Med Biol. 2013;58(1):N1–12.
5. Kang J, Kim EK, Kim GR, et al. Photoacoustic imaging of breast microcalcifications: a validation study with 3-dimensional ex vivo data and spectrophotometric measurement. J Biophotonics. 2015;8(1–2):71–80.
6. Kang J, Chang JH, Wilson BC, et al. A prototype hand-held trimodal instrument for in vivo ultrasound, photoacoustic, and fluorescence imaging. Rev Sci Instrum. 2015;86(3):034901.
7. Moon H, Kumar D, Kim H, et al. Amplified photoacoustic performance and enhanced photothermal stability of reduced graphene oxide coated gold nanorods for sensitive photo acoustic imaging. ACS Nano. 2015;9(3):2711–9.
8. Ju KY, Kang J, Pyo J, et al. pH-Induced aggregated melanin nanoparticles for photoacoustic signal amplification. Nanoscale. 2016;8(30):14448–56.
9. Lee J, Chang JH, Jeong JS, et al. Backscattering measurement from a single microdroplet. IEEE Trans Ultrason Ferroelectr Freq Control. 2011;58(4):874–9.
10. Hwang JY, Kim J, Park JM, et al. Cell deformation by singlebeam acoustic trapping: a promising tool for measurements of cell mechanics. Sci Rep. 2016;6:27238.
11. Yoon S, Kim MG, Chiu CT, et al. Direct and sustained intracellular delivery of exogenous molecules using acoustic-transfection with high frequency ultrasound. Sci Rep. 2016;6:20477.
12. Song JH, Yoo Y, Song TK, et al. Real-time monitoring of HIFU treatment using pulse inversion. Phys Med Biol. 2013;58(15):5333–50.
13. Kim H, Kang J, Chang JH. Thermal therapeutic method for selective treatment of deep-lying tissue by combining laser and high-intensity focused ultrasound energy. Opt Lett. 2014;39(9):2806–9.
14. Ebbini ES, Ter Haar G. Ultrasound-guided therapeutic focused ultrasound: current status and future directions. Int J Hyperth. 2015;31(2):77–89.
15. Feinstein SB. The evolution of contrast ultrasound from diagnosis to therapy. J Am Coll Cardiol. 2016;67(21):2516–8.
16. Blomley MJK, Cooke JC, Unger EC, et al. Science, medicine, and the future—microbubble contrast agents: a new era in ultrasound. Br Med J. 2001;322(7296):1222–5.
17. Garg S, Thomas AA, Borden MA. The effect of lipid monolayer in-plane rigidity on in vivo microbubble circulation persistence. Biomaterials. 2013;34(28):6862–70.
18. Chen JL, Dhanaliwala AH, Dixon AJ, et al. Synthesis and characterization of transiently stable albumin-coated microbubbles via a flow-focusing microfluidic device. Ultrasound Med Biol. 2014;40(2):400–9.
19. Song S, Guo HZ, Jiang ZQ, et al. Self-assembled microbubbles as contrast agents for ultrasound/magnetic resonance dual-modality imaging. Acta Biomater. 2015;24:266–78.
20. Grinstaff MW, Suslick KS. Air-filled proteinaceous microbubbles—synthesis of an echo-contrast agent. Proc Natl Acad Sci USA. 1991;88(17):7708–10.
21. Carroll BA, Turner RJ, Tickner EG, et al. Gelatin encapsulated nitrogen microbubbles as ultrasonic contrast agents. Invest Radiol. 1980;15(3):260–6.
22. Moon H, Yoon C, Lee TW, et al. Therapeutic ultrasound contrast agents for the enhancement of tumor diagnosis and tumor therapy. J Biomed Nanotechnol. 2015;11(7):1183–92.
23. Yang F, Li Y, Chen Z, et al. Superparamagnetic iron oxide nanoparticle-embedded encapsulated microbubbles as dual contrast agents of magnetic resonance and ultrasound imaging. Biomaterials. 2009;30(23):3882–90.
24. Postema M, Van Wamel A, Lancée CT, et al. Ultrasound-induced encapsulated microbubble phenomena. Ultrasound Med Biol. 2004;30(6):827–40.
25. Miller DL. Frequency relationships for ultrasonic activation of free microbubbles, encapsulated microbubbles, and gas-filled micropores. J Acoust Soc Am. 1998;104(4):2498–505.
26. Maresca G, Summaria V, Colagrande C, et al. New prospects for ultrasound contrast agents. Eur J Radiol. 1998;27:S171–8.
27. Schuh S, Chan K, Langer JC, et al. Properties of serial ultrasound clinical diagnostic pathway in suspected appendicitis and related computed tomography use. Acad Emerg Med. 2015;22(4):406–14.
28. Walton CB, Shohet RV. Tiny bubbles and endocytosis? Circ Res. 2009;104(5):563–5.
29. Sirsi SR, Borden MA. Advances in ultrasound mediated gene therapy using microbubble contrast agents. Theranostics. 2012;2(12):1208–22.
30. Mehier-Humbert S, Bettinger T, Yan F, et al. Plasma membrane poration induced by ultrasound exposure: implication for drug delivery. J Control Release. 2005;104(1):213–22.
31. Tsutsui JM, Xie F, Porter RT. The use of microbubbles to target drug delivery. Cardiovasc Ultrasound. 2004;2(1):1.
32. Unger EC, Porter T, Culp W, et al. Therapeutic applications of lipid-coated microbubbles. Adv Drug Deliv Rev. 2004;56(9):1291–314.
33. Unger EC, Hersh E, Vannan M, et al. Local drug and gene delivery through microbubbles. Prog Cardiovasc Dis. 2001;44(1):45–54.
34. Moon H, Kang J, Sim C, et al. Multifunctional theranostic contrast agent for photoacoustics- and ultrasound-based tumor diagnosis and ultrasound-stimulated local tumor therapy. J Control Release. 2015;218:63–71.
35. Rawat M, Singh D, Saraf S, et al. Lipid carriers: A versatile delivery vehicle for proteins and peptides. Yakugaku Zasshi J Pharm Soc Jpn. 2008;128(2):269–80.
36. Hernot S, Klibanov AL. Microbubbles in ultrasound-triggered drug and gene delivery. Adv Drug Deliv Rev. 2008;60(10):1153–66.

37. Cullen DM, Breidahl WH, Janes GC. Diagnostic accuracy of shoulder ultrasound performed by a single operator. Australas Radiol. 2007;51(3):226–9.

38. Fan Z, Kumon RE, Deng CX. Mechanisms of microbubble-facilitated sonoporation for drug and gene delivery. Ther Deliv. 2014;5(4):467–86.

39. Borden MA, Kruse DE, Caskey CF, et al. Influence of lipid shell physicochemical properties on ultrasound-induced microbubble destruction. IEEE Trans Ultrason Ferroelectr Freq Control. 2005;52(11):1992–2002.

40. Blomley MJ, Cooke JC, Unger EC, et al. Microbubble contrast agents: a new era in ultrasound. BMJ. 2001;322(7296):1222–5.

41. Ferrara K, Pollard R, Borden M. Ultrasound microbubble contrast agents: fundamentals and application to gene and drug delivery. Biomed Eng. 2007;9:415–47.

42. Klibanov AL. Preparation of targeted microbubbles: ultrasound contrast agents for molecular imaging. Med Biol Eng Comput. 2009;47(8):875–82.

43. Ernst H, Hahn EG, Balzer T, et al. Color doppler ultrasound of liver lesions: signal enhancement after intravenous injection of the ultrasound contrast agent Levovist. J Clin Ultrasound. 1996;24(1):31–5.

44. Faez T, Goertz D, De Jong N. Characterization of definity^{TM} ultrasound contrast agent at frequency range of 5–15 MHz. Ultrasound Med Biol. 2011;37(2):338–42.

45. Li TL, Tachibana K, Kuroki M, et al. Gene transfer with echo-enhanced contrast agents: comparison between Albunex, Optison, and Levovist in mice—initial results. Radiology. 2003; 229(2):423–8.

46. Watanabe R, Matsumura M, Chen CJ, et al. Characterization of tumor imaging with microbubble-based ultrasound contrast agent, Sonazoid, in rabbit liver (vol 28, pg 973, 2006). Biol Pharm Bull. 2006;29(12):2536.

47. von Herbay A, Vogt C, Haussinger D. Late-phase pulse-inversion sonography using the contrast agent Levovist: differentiation between benign and malignant focal lesions of the liver. Am J Roentgenol. 2002;179(5):1273–9.

48. Schwarz KQ, Chen XC, Steinmetz S, et al. Harmonic imaging with Levovist. J Am Soc Echocardiogr. 1997;10(1):1–10.

49. Yanagisawa K, Moriyasu F, Miyahara T, et al. Phagocytosis of ultrasound contrast agent microbubbles by Kupffer cells. Ultrasound Med Biol. 2007;33(2):318–25.

50. Ward M, Wu JR, Chiu JF. Experimental study of the effects of Optison® concentration on sonoporation in vitro. Ultrasound Med Biol. 2000;26(7):1169–75.

51. Lindner JR, Dayton PA, Coggins MP, et al. Noninvasive imaging of inflammation by ultrasound detection of phagocytosed microbubbles. Circulation. 2000;102(5):531–8.

52. Sontum PC. Physicochemical characteristics of Sonazoid^{TM}, a new contrast agent for ultrasound imaging. Ultrasound Med Biol. 2008;34(5):824–33.

53. Appis AW, Tracy MJ, Feinstein SB. Update on the safety and efficacy of commercial ultrasound contrast agents in cardiac applications. Echo research and practice. 2015;2(2):R55–62.

54. Bokor D, Chambers JB, Rees PJ, et al. Clinical safety of SonoVue^{TM}, a new contrast agent for ultrasound imaging, in healthy volunteers and in patients with chronic obstructive pulmonary disease. Invest Radiol. 2001;36(2):104–9.

55. Morel DR, Schwieger I, Hohn L, et al. Human pharmacokinetics and safety evaluation of SonoVue^{TM}, a new contrast agent for ultrasound imaging. Invest Radiol. 2000;35(1):80–5.

56. Schneider M. Characteristics of SonoVue^{TM}. Echocardiogr J Cardiovas Ultrasound Allied Tech. 1999;16(7):743–6.

57. Gorce JM, Arditi M, Schneider M. Influence of bubble size distribution on the echogenicity of ultrasound contrast agents—a study of SonoVue^{TM}. Invest Radiol. 2000;35(11):661–71.

58. Datta S, Coussics CC, Ammi AY, et al. Ultrasound-enhanced thrombolysis using Definity® as a cavitation nucleation agent. Ultrasound Med Biol. 2008;34(9):1421–33.

59. Miyamoto Y, Ito T, Takada E, et al. Efficacy of sonazoid (perflubutane) for contrast-enhanced ultrasound in the differentiation of focal breast lesions: phase 3 multicenter clinical trial. Am J Roentgenol. 2014;202(4):W400–7.

60. Raisinghani A, DeMaria AN. Physical principles of microbubble ultrasound contrast agents. Am J Cardiol. 2002;90(10A):3J–7J.

61. Gramiak R, Shah PM, Kramer DH. Ultrasound cardiography: contrast studies in anatomy and function. Radiology. 1969; 92(5):939–48.

62. Hoff L. Acoustic characterization of contrast agents for medical ultrasound imaging. Berlin: Springer; 2001.

63. Eloubeidi MA, Chen VK, Eltoum IA, et al. Endoscopic ultrasound-guided fine needle aspiration biopsy of patients with suspected pancreatic cancer: diagnostic accuracy and acute and 30-day complications. Am J Gastroenterol. 2003;98(12):2663–8.

64. Defreitas R, Costa MV, Schneider SV, et al. Accuracy of ultrasound and clinical examination in the diagnosis of axillary lymph-node metastases in breast-cancer. Eur J Surg Oncol. 1991;17(3):240–4.

65. Villanueva FS, Wagner WR. Ultrasound molecular imaging of cardiovascular disease. Nat Clin Pract Cardiovasc Med =. 2008;5:S26–32.

66. Desser TS, Jeffrey RB. Tissue harmonic imaging techniques: physical principles and clinical applications. Semin Ultrasound CT MRI. 2001;22(1):1–10.

67. Song J, Chang JH, Song TK, et al. Coded tissue harmonic imaging with nonlinear chirp signals. Ultrasonics. 2011;51(4): 516–21.

68. Bouakaz A, Frigstad S, Ten Cate FJ, et al. Super harmonic imaging: a new imaging technique for improved contrast detection. Ultrasound Med Biol. 2002;28(1):59–68.

69. Kono Y, Moriyasu F, Mine Y, et al. Gray-scale second harmonic imaging of the liver with galactose-based microbubbles. Invest Radiol. 1997;32(2):120–5.

70. Unger EC, Matsunaga TO, McCreery T, et al. Therapeutic applications of microbubbles. Eur J Radiol. 2002;42(2):160–8.

71. Church CC, Carstensen EL. "Stable" inertial cavitation. Ultrasound Med Biol. 2001;27(10):1435–7.

72. Ohl CD, Wolfrum B. Detachment and sonoporation of adherent HeLa-cells by shock wave-induced cavitation. Biochim Biophys Acta. 2003;1624(1–3):131–8.

73. Lentacker I, De Cock I, Deckers R, et al. Understanding ultrasound induced sonoporation: definitions and underlying mechanisms. Adv Drug Deliv Rev. 2014;72:49–64.

74. Doinikov AA, Bouakaz A. Theoretical investigation of shear stress generated by a contrast microbubble on the cell membrane as a mechanism for sonoporation. J Acoust Soc Am. 2010; 128(1):11–9.

75. Fan Z, Kumon RE, Deng CX. Mechanisms of microbubble-facilitated sonoporation for drug and gene delivery. Ther Deliv. 2014;5(4):467–86.

76. Zhao YZ, Luo YK, Lu CT, et al. Phospholipids-based microbubbles sonoporation pore size and reseal of cell membrane cultured in vitro. J Drug Target. 2008;16(1):18–25.

77. Tsunoda S, Mazda O, Oda Y, et al. Sonoporation using microbubble BR14 promotes pDNA/siRNA transduction to murine heart. Biochem Biophys Res Commun. 2005;336(1):118–27.

78. Sirsi S, Borden M. Microbubble compositions, properties and biomedical applications. Bubble Sci Eng Technol. 2009;1(1–2): 3–17.

79. Kooiman K, Foppen-Harteveld M, van der Steen AFW, et al. Sonoporation of endothelial cells by vibrating targeted microbubbles. J Control Release. 2011;154(1):35–41.

80. Karshafian R, Samac S, Bevan PD, et al. Microbubble mediated sonoporation of cells in suspension: clonogenic viability and influence of molecular size on uptake. Ultrasonics. 2010; 50(7):691–7.

81. Liao AH, Ho HC, Lin YC, et al. Effects of microbubble size on ultrasound-induced transdermal delivery of high-molecular-weight drugs. PLoS ONE. 2015;10(9):e0138500.

82. Cordon-Cardo C, O'Brien JP, Casals D, et al. Multidrug-resistance gene (P-glycoprotein) is expressed by endothelial cells at blood–brain barrier sites. Proc Natl Acad Sci. 1989;86(2):695–8.

83. Tung YS, Vlachos F, Feshitan JA, et al. The mechanism of interaction between focused ultrasound and microbubbles in blood–brain barrier opening in mice. J Acoust Soc Am. 2011;130(5):3059–67.

84. Yang FY, Fu WM, Chen WS, et al. Quantitative evaluation of the use of microbubbles with transcranial focused ultrasound on blood–brain-barrier disruption. Ultrason Sonochem. 2008;15(4): 636–43.

85. Hynynen K, McDannold N, Vykhodtseva N, et al. Non-invasive opening of BBB by focused ultrasound. Acta Neurochir Suppl. 2003;86:555–8.

86. Samiotaki G, Karakatsani ME, Buch A, et al. Pharmacokinetic analysis and drug delivery efficiency of the focused ultrasound-induced blood–brain barrier opening in non-human primates. Magn Reson Imaging. 2016;37:273–81.

87. Cho H, Lee HY, Han M, et al. Localized down-regulation of P-glycoprotein by focused ultrasound and microbubbles induced blood–brain barrier disruption in rat brain. Sci Rep. 2016;6: 31201.

88. Bai M, Shen M, Teng Y, et al. Enhanced therapeutic effect of Adriamycin on multidrug resistant breast cancer by the ABCG2-siRNA loaded polymeric nanoparticles assisted with ultrasound. OncoTarget. 2015;6:43779–90.

89. Baron Toaldo M, Salvatore V, Marinelli S, et al. Use of VEGFR-2 targeted ultrasound contrast agent for the early evaluation of response to sorafenib in a mouse model of hepatocellular carcinoma. Mol Imaging Biol. 2015;17(1):29–37.

90. Shen ZY, Xia GL, Wu MF, et al. The effects of percutaneous ethanol injection followed by 20-kHz ultrasound and microbubbles on rabbit hepatic tumors. J Cancer Res Clin Oncol. 2016;142(2):373–8.

91. Zhang Y, Chang R, Li M, et al. Docetaxel-loaded lipid microbubbles combined with ultrasound-triggered microbubble destruction for targeted tumor therapy in MHCC-H cells. Onco Targets Ther. 2016;9:4763–71.

92. Kotopoulis S, Delalande A, Popa M, et al. Sonoporation-enhanced chemotherapy significantly reduces primary tumour burden in an orthotopic pancreatic cancer xenograft. Mol Imaging Biol. 2014;16(1):53–62.

93. Xing LX, Shi QS, Zheng KL, et al. Ultrasound-mediated microbubble destruction (UMMD) facilitates the delivery of CA19-9 targeted and paclitaxel loaded mPEG-PLGA-PLL nanoparticles in pancreatic cancer. Theranostics. 2016;6(10): 1573–87.

94. Sorace AG, Saini R, Mahoney M, et al. Molecular ultrasound imaging using a targeted contrast agent for assessing early tumor response to antiangiogenic therapy. J Ultrasound Med. 2012; 31(10):1543–50.

95. Staud F, Pavek P. Breast cancer resistance protein (BCRP/ABCG2). Int J Biochem Cell Biol. 2005;37(4):720–5.

96. Schinkel AH, Jonker JW. Mammalian drug efflux transporters of the ATP binding cassette (ABC) family: an overview. Adv Drug Deliv Rev. 2003;55:3–29.

97. Adams H. Guidelines for the early management of patients with ischemic stroke: 2005 guidelines update: a scientific statement from the stroke council of the American Heart Association/American Stroke Association" (vol 36, pg 916, 2005). Stroke. 2006;37(6):1582.

98. Go AS. Heart disease and stroke statistics-2013 update: a report from the American Heart Association (vol 127, pg e6, 2013). Circulation. 2013;127(23):E841.

99. Unger E, Porter T, Lindner J, et al. Cardiovascular drug delivery with ultrasound and microbubbles. Adv Drug Deliv Rev. 2014;72:110–26.

100. Wang XW, Gkanatsas Y, Palasubramaniam J, et al. Thrombus-targeted theranostic microbubbles: a new technology towards concurrent rapid ultrasound diagnosis and bleeding-free fibrinolytic treatment of thrombosis. Theranostics. 2016;6(5): 726–38.

101. Hagisawa K, Nishioka T, Suzuki R, et al. Thrombus-targeted perfluorocarbon-containing liposomal bubbles for enhancement of ultrasonic thrombolysis: invitro and invivo study. J Thromb Haemost. 2013;11(8):1565–73.

102. Schutt EG, Klein DH, Mattrey RM, et al. Injectable microbubbles as contrast agents for diagnostic ultrasound imaging: the key role of perfluorochemicals. Angew Chem Int Ed. 2003; 42(28):3218–35.

103. Shekhar H, Rychak JJ, Doyley MM. Modifying the size distribution of microbubble contrast agents for high-frequency subharmonic imaging. Med Phys. 2013;40(8):082903.

104. Feshitan JA, Chen CC, Kwan JJ, et al. Microbubble size isolation by differential centrifugation. J Colloid Interface Sci. 2009;329(2):316–24.

105. Hettiarachchi K, Talu E, Longo ML, et al. On-chip generation of microbubbles as a practical technology for manufacturing contrast agents for ultrasonic imaging. Lab Chip. 2007;7(4):463–8.

106. de Jong N, Bouakaz A, Frinking P. Basic acoustic properties of microbubbles. Echocardiography. 2002;19(3):229–40.

107. Hannah A, Luke G, Wilson K, et al. Indocyanine green-loaded photoacoustic nanodroplets: dual contrast nanoconstructs for enhanced photoacoustic and ultrasound imaging. ACS Nano. 2014;8(1):250–9.

108. Min KH, Min HS, Lee HJ, et al. pH-controlled gas-generating mineralized nanoparticles: a theranostic agent for ultrasound imaging and therapy of cancers. ACS Nano. 2015;9(1):134–45.

109. Tay LM, Xu C. Coating microbubbles with nanoparticles for medical imaging and drug delivery. Nanomedicine. 2017;12(2): 91–4.

110. Li J, Tian Y, Shan D, et al. Neuropeptide YY 1 receptor-mediated biodegradable photoluminescent nanobubbles as ultrasound contrast agents for targeted breast cancer imaging. Biomaterials. 2016;116:106–17.